Wu et al. *Zool. Res.* 2026, 47(1): 117−127
https://doi.org/10.24272/j.issn.2095-8137.2025.088
https://cstr.cn/32248.14.zr.2025.088

ZR | Zoological Research

Article Open Access

Molecular divergence of *TRPA1* in cetaceans supports lineage-specific adaptation to aquatic life

Tian-Zhen Wu[1], Xian-Ting Huang[2], Yu-Qing Deng[2], Luo-Ying Deme[2], Shi-Xia Xu[2,*], Guang Yang[1,2,*]

[1] *Southern Marine Science and Engineering Guangdong Laboratory (Guangzhou)*, *Guangzhou*, *Guangdong* 511458, *China*
[2] *Jiangsu Key Laboratory for the Biodiversity Conservation and Sustainable Utilization in the Middle and Lower Reaches of the Yangtze River Basin*, *College of Life Sciences*, *Nanjing Normal University*, *Nanjing*, *Jiangsu* 210023, *China*

ABSTRACT

Gene loss represents a powerful driver of adaptive evolution. Cetaceans, which underwent a profound transition from terrestrial to fully aquatic life, provide an excellent model for investigating this process. Comparative genomic analysis of the cold-sensitive ion channel transient receptor potential ankyrin 1 (*TRPA1*) revealed lineage-specific patterns of degeneration across cetaceans. In toothed whales, the ancestral lineage exhibited extensive exon loss within the *TRPA1* locus, whereas baleen whales showed signatures consistent with markedly reduced or absent *TRPA1* expression. These molecular alterations were inferred to disrupt or abolish *TRPA1* protein function across cetaceans. Integration of these findings with established experimental evidence from human and murine TRPA1 studies supported several adaptive hypotheses for *TRPA1* gene loss, including tolerance to abrupt thermal fluctuations, attenuation of nociceptive responses in aquatic environments, specialization of integumentary sensory systems, and the emergence of echolocation-associated sensory trade-offs in toothed whales. Collectively, these findings expand the gene loss repertoire of cetaceans and provide novel insights into the molecular underpinnings of secondary aquatic adaptation in mammals.

Keywords: Cetacean; Gene loss; *TRPA1*; Molecular evolution; Evolutionary adaptation

INTRODUCTION

Cetaceans, descended from terrestrial artiodactyls in the Indo-Pakistan region approximately 52.5 million years ago (Ma), represent a fully aquatic lineage that has undergone profound morphological, physiological, and behavioral remodeling (Uhen, 2010). Adaptations such as hydrodynamic body shaping, enhanced thermoregulatory mechanisms, reorganization of auditory structures, simplification of integumentary architecture, and remodeling of sensory modalities facilitated the occupation of diverse marine environments and supported extensive ecological radiation (Chai et al., 2024; Gai et al., 2023; Guo et al., 2024; Huang et al., 2021; Liang et al., 2022; Wu et al., 2022; Xu et al., 2025; Yu et al., 2021; Zhang et al., 2025; Zhou et al., 2022). These evolutionary transformations position cetaceans as a valuable model for studying the genomic basis of adaptive transitions from terrestrial to aquatic life. In the context of historical and ongoing climate fluctuations, analysis of cetacean molecular responses to environmental stress offers critical insights into mammalian resilience and adaptation to extreme conditions.

Gene loss is increasingly recognized as a major evolutionary force driving adaptive evolution in cetaceans. Advances in genomic sequencing have enabled the identification of numerous lineage-specific gene inactivations tightly linked to ecological and physiological shifts associated with aquatic specialization (Huelsmann et al., 2019). Losses of genes involved in chemosensory function, such as *OMACS*, *NQO1*, *TAS1R*, and *TAS2R*, correlate with diminished olfactory and gustatory capabilities (Feng et al., 2014; Kishida et al., 2015). Similarly, pseudogenization of enamel-related genes, such as *ACP4*, *KLK4*, *MMP20*, and *ACPT*, supports the progressive degeneration of dentition in baleen whales (Mu et al., 2021; Randall et al., 2022). Disruption of sebum-producing genes (*DGAT2L6* and *AWAT1*) and epidermal keratin genes (*KRT1* and *KRT2*) further indicates adaptation of the skin to aquatic environments (Lopes-Marques et al., 2019; Springer et al., 2021). A recent survey cataloged 1 866 gene loss events across 57 cetacean species, underscoring the extensive genomic remodeling accompanying aquatic life (Themudo et al., 2025). Systematic reconstruction of the evolutionary trajectories of pseudogenes in cetaceans can deepen our understanding of the molecular mechanisms

Received: 09 July 2025; Accepted: 15 September 2025; Online: 16 September 2025

Foundation items: This work was supported by the National Natural Science Foundation of China (32030011, U24A20362, 32070409), Qing Lan Project of Jiangsu Province, Priority Academic Program Development of Jiangsu Higher Education Institutions, and PI Project of Southern Marine Science and Engineering Guangdong Laboratory (Guangzhou) (GML2021GD0805)

*Corresponding authors, E-mail: xushixia78@163.com; gyang@njnu.edu.cn

underlying phenotypic evolution and elucidate the genetic pathways through which mammals adapt to novel ecological niches.

Transient receptor potential ankyrin 1 (*TRPA1*) is a polymodal ion channel expressed across a broad range of neuronal and non-neuronal cell types. Within the peripheral nervous system, it localizes to sensory ganglia, including dorsal root (DRG), trigeminal (TG), and nodose ganglia, as well as astrocytes, cochlear hair cells, cardiac ventricular myocytes, respiratory epithelial cells, and multiple immune cell types (Zhang et al., 2022). Like other temperature-sensitive ion channels, *TRPA1* converts thermal stimuli into electrical signals that are relayed to the central nervous system, thereby contributing to thermal perception (Delmas et al., 2011; Vriens et al., 2014). *TRPA1* exhibits considerable functional diversity across animal lineages. In invertebrates, its thermal gating properties range from heat activation in species such as planarians, mites, flies, mosquitoes, and honeybees, to cold sensitivity in *Caenorhabditis elegans* (Chen, 2015; Zhang et al., 2022). In mammals, *TRPA1* thermosensitivity remains unresolved, with divergent findings across both species and experimental systems. Notably, Zhang et al. (2022) systematically analyzed 27 studies that examined *TRPA1* temperature sensitivity in various species, including humans, rhesus monkeys, mice, rats, and thirteen-lined ground squirrels, using expression platforms ranging from primary sensory neurons to heterologous systems such as HEK293 cells, oocytes, neuroblastoma cells, tumor cells, and planar lipid bilayers. Among these studies, 16 reported cold-induced activation, seven found no thermal responses, three detected sensitivities to both cold and heat, and one observed heat activation alone. These findings indicate no consistent pattern across taxa or experimental system, highlighting persistent uncertainty regarding TRPA1 thermal gating in mammals.

Beyond thermosensation, *TRPA1* mediates a wide range of physiological and pathophysiological processes. It functions as a chemosensor for electrophilic compounds such as allyl isothiocyanate and allicin, detecting both environmental irritants (e.g., acrolein) and endogenous proalgesic agents (Bautista et al., 2006; Kwan et al., 2006). *TRPA1* also contributes to mechanical nociception, particularly under inflammatory conditions that potentiate pain hypersensitivity (Kwan et al., 2006; Nilius et al., 2012), and is implicated in visceral pain signaling (Balemans et al., 2017) and migraine generation (Benemei et al., 2014). It functions as a sensor of oxidative stress by detecting reactive oxygen species, thereby supporting cellular defense responses (Andersson et al., 2008), and is required for chronic itch signaling under pathological conditions (Moore et al., 2018; Wilson et al., 2013). In the auditory system, *TRPA1* modulates cochlear function by adjusting auditory sensitivity following acoustic trauma (Nagata et al., 2005; Vélez-Ortega et al., 2023). In skin, *TRPA1* regulates epidermal barrier integrity, keratinocyte differentiation, and immune activity, thereby contributing to the pathophysiology of various inflammatory and neoplastic dermatologic conditions (Maglie et al., 2021). Structurally, *TRPA1* is composed of approximately 1 100 amino acids, with intracellular N- and C-termini. The N-terminal domain contains 14–18 ankyrin repeat motifs, followed by six transmembrane segments. Among these, the fifth and sixth segments form the pore region, which is essential for calcium ion transport and extracellular signal transduction (Meents et al., 2019). These architectural features are fundamental to *TRPA1* channel activity.

Thermal adaptation of *TRPA1* has been documented across multiple species. In hot spring snakes, specific coding mutations in *TRPA1* enhance channel sensitivity to elevated temperatures, facilitating thermal detection in high-temperature habitats (Yan et al., 2022). In infrared-sensing species such as pythons and pit vipers, convergent amino acid substitutions in *TRPA1* have evolved independently and are thought to mediate infrared signal detection (Geng et al., 2011; Gracheva et al., 2010). In amphibians, alternative splicing modulates *TRPA1*-mediated thermosensitivity by introducing a valine residue at position 277 between the sixth and seventh ankyrin repeats, thereby increasing the heat activation threshold of the TRPA1 protein (Saito et al., 2022). In mammals, a single residue within the fifth transmembrane domain—glycine (G878) in rodents versus valine (V875) in primates—accounts for the observed interspecific differences in cold sensitivity (Chen et al., 2013). Collectively, these findings underscore the functional and structural plasticity of *TRPA1* under divergent thermal selective pressures.

Despite the extensive functional diversity of *TRPA1* in mammals, patterns of sequence evolution in cetaceans remain largely unexplored. The present study characterized evolutionary modifications of *TRPA1* across cetacean lineages and explored potential molecular adaptations associated with the secondary transition from terrestrial to aquatic environments. Understanding these evolutionary mechanisms will provide valuable insights into how sensory genes adapt to extreme environmental conditions, thereby advancing our understanding of the molecular basis of aquatic adaptation in mammals.

MATERIALS AND METHODS

Sequence acquisition and alignment

A comprehensive dataset of *TRPA1* coding sequences was assembled, comprising 27 cetacean species, including 19 toothed whales and eight baleen whales, alongside 28 additional mammalian species spanning 12 major placental orders (Supplementary Table S1). Cetacean taxa included representatives from three mysticete families (Balaenidae, Balaenopteridae, and Eschrichtiidae) and 10 odontocete families (Delphinidae, Iniidae, Kogiidae, Lipotidae, Monodontidae, Phocoenidae, Physeteridae, Platanistidae, Pontoporiidae, and Ziphiidae). The comparative mammalian dataset comprised 25 families, including Elephantidae, Trichechidae, Cercopithecidae, Hominidae, Cricetidae, Muridae, Erinaceidae, Soricidae, Bovidae, Suidae, Camelidae, Cervidae, Hippopotamidae, Canidae, Odobenidae, Otariidae, Phocidae, Ursidae, Phyllostomidae, Vespertilionidae, Equidae, Rhinocerotidae, Manidae, Dasypodidae, and Choloepodidae. Initial retrieval of *TRPA1* coding sequences was performed through batch Entrez queries in the NCBI genome database (https://www.ncbi.nlm.nih.gov/). For taxa lacking annotated genomes, BLAST searches (Altschul et al., 1990) were conducted using orthologous sequences from humans, cattle, or closely related species as queries. Preliminary alignments were generated using MUSCLE implemented in MEGA7 (Edgar, 2004; Kumar et al., 2016), and sequence completeness was assessed manually. Subsequently, complete sequences were realigned using PRANK (Löytynoja, 2013). Regions with ambiguous homology, extensive gaps, or poor alignment quality were excluded using Gblocks v.0.91b

(Castresana, 2000) with the parameters -t=c and -b5=h.

Identification of inactivating mutations

To assess coding sequence integrity, putative inactivating mutations in *TRPA1* were identified, including disruptions to initiation or stop codons, frameshift-inducing insertions or deletions, premature stop codons, and splice site mutations at intron-exon boundaries (GT/AG). Candidate mutations were validated by aligning assembled sequences to raw sequencing reads stored in the Sequence Read Archive (Kodama et al., 2012), allowing exclusion of errors introduced during genome assembly. Illumina-generated sequencing datasets included muscle-derived reads from the Indo-Pacific humpback dolphin (*Sousa chinensis*, SRR14018396) and Antarctic minke whale (*Balaenoptera bonaerensis*, SRR4011114) and skin tissue of the gray whale (*Eschrichtius robustus*, SRR13562679) and Indus River dolphin (*Platanista minor*, SRR11431927). For mutations shared across multiple cetacean lineages, validation was performed using PCR amplification. To assess the presence of large fragment deletions, comparative genomic alignments from 120 and 470 mammal datasets were examined using the UCSC Genome Browser (https://genome.ucsc.edu/cgi-bin/hgTracks?db=hg38) (Hecker & Hiller, 2020; Minkin & Salzberg, 2025). Sequences potentially involved in regulatory functions were further investigated using the ReMap (https://remap.univ-amu.fr/) and ENCODE (https://www.encodeproject.org/) databases.

Validation of inactivating mutations by polymerase chain reaction (PCR)

Five inactivating mutations (Supplementary Table S2) were validated in two cetacean species: the common minke whale (*Balaenoptera acutorostrata*) and Yangtze finless porpoise (*Neophocaena asiaeorientalis*), both recovered as stranded individuals from the East China Sea and the Yangtze River, respectively. Primers were designed using Primer-BLAST (https://www.ncbi.nlm.nih.gov/tools/primer-blast) and are listed in Supplementary Table S2. Genomic DNA was extracted from muscle tissue using a DNeasy Blood & Tissue Kit (Qiagen, Germany) according to the manufacturer's protocols. PCR amplification was conducted in 50 μL reaction volumes using standard reagents and cycling conditions, as detailed in the Supplementary Materials. Amplified products were sequenced using the Illumina platform (USA), and the resulting data were visualized using SnapGene Viewer v.6.2.2 to verify the presence of inactivating mutations.

Querying *TRPA1* in transcriptome data

To assess whether inactivating mutations affected *TRPA1* transcription, transcriptomic datasets from 15 tissue samples representing four baleen whale species were analyzed for evidence of gene expression (Supplementary Table S3). The species included the blue whale (*Balaenoptera musculus*) (Bukhman et al., 2024; Lopes-Marques et al., 2019), bowhead whale (*Balaena mysticetus*) (Keane et al., 2015), common minke whale (Yim et al., 2014), and humpback whale (*Megaptera novaeangliae*) (Geoghegan et al., 2018; Tollis et al., 2019; Tsagkogeorga et al., 2015). Transcriptome reads were queried using the nucleotide BLAST tool (https://blast.ncbi.nlm.nih.gov/Blast.cgi), with alignments mapped to the *TRPA1* coding sequence to evaluate transcriptional activity. As comparative controls, transcriptomic data from the hippopotamus (*Hippopotamus amphibius*) (Figuet et al., 2021), a close relative of cetaceans, as well as cattle (*Bos taurus*) (Hou et al., 2022) and humans (*Homo sapiens*) (Horwitz et al., 2024) were also screened for *TRPA1* expression.

Selection pressure analysis

Comparative analysis revealed that toothed whales have lost the *TRPA1* coding region corresponding to the transmembrane domain, preventing the formation of a functional protein. In contrast, baleen whales have retained the full-length *TRPA1* sequence, although the nature and extent of selection pressures acting on these lineages remain unclear. To evaluate selective constraints on the *TRPA1* gene in baleen whales, an aligned sequence dataset comprising 3 357 bp was analyzed using two complementary approaches: PAML and RELAX. The ratio of nonsynonymous to synonymous substitution rates ($\omega=d_N/d_S$) was used to evaluate selective pressure, with $\omega>1$, $=1$, and <1 indicating positive, neutral, and purifying selection, respectively. Codon-based maximum-likelihood estimates of ω were calculated using Codeml in PAML v.4.9e (Yang, 2007). Three branch models were tested: (a) a one-ratio model assuming uniform ω across all branches (null hypothesis); (b) a two-ratio model allowing different ω values for the foreground and background branches (alternative hypothesis); and (c) a modified version of model b with ω in the foreground branches fixed at 1. Model fit was assessed via likelihood ratio tests (LRTs). A significantly better fit of model (b) over model (a), but not over model (c), was interpreted as evidence of relaxed selection in the foreground lineages. Phylogenetic relationships between baleen whales and other mammals (excluding toothed whales) were based on McGowen et al. (2020) and TimeTree (https://timetree.org/) and were used as the input tree for PAML analyses. Given the potential functionality of GC splice sites (Burset et al., 2000; Churbanov et al., 2008; Hiller et al., 2006), the fin whale (*Balaenoptera physalus*), gray whale, and Antarctic minke whale were classified as carrying inactivating mutations, while the remaining five baleen whale species were classified as lineages with intact sequences. Each group was designated as the foreground in separate branch model tests using PAML, with all other lineages in the phylogenetic tree treated as background.

RELAX analysis (Wertheim et al., 2015) was conducted via the Datamonkey web platform (https://datamonkey.org/). This method estimates a selection intensity parameter (K), where a value greater than 1 indicates intensified selection pressure, and a value less than 1 suggests relaxed selection pressure. In the null model, K is assumed to be 1, with three ω values and corresponding site class proportions estimated jointly for test and reference branches. In the alternative model, K is treated as a free parameter, and three ω values and their site proportions are calculated separately for the test and reference branches. Statistical significance was determined by comparing models via LRT. An inferred shift in ω toward neutrality (i.e., approaching 1) in test branches relative to reference branches was interpreted as evidence of relaxed selective constraint. Foreground and background designations followed the same grouping scheme used in the PAML analysis.

RESULTS

***TRPA1* in toothed whales**

Extensive exon loss was identified in *TRPA1* across toothed

whale lineages (Figure 1). Deletions spanning exons 2 through 23 were consistently observed in all sampled toothed whales, except the Indus River dolphin. BLAST-based searches further revealed that the last two exons were absent in the Amazon River dolphin (*Inia geoffrensis*), the last three exons were missing in the La Plata dolphin (*Pontoporia blainvillei*), and no exons were detected in the pygmy sperm whale (*Kogia breviceps*).

Synteny analyses of the *TRPA1* gene and its flanking regions were conducted across 43 representative mammalian species from the Euarchontoglires, Laurasiatheria, Xenarthra, and Afrotheria superorders (Figure 2), as well as a broader dataset comprising 470 mammals, including 25 toothed whales (Supplementary Figure S1). These analyses corroborated the BLAST results, revealing large segmental deletions in all examined toothed whale genomes. Notably, the pygmy sperm whale lacked the entire *TRPA1* gene region, whereas the Indus River dolphin retained the genomic segment covering exons 2 to 12.

Several lineage-specific inactivating mutations were also identified. A 19 bp deletion in exon 1 and a 4 bp deletion in exon 27 were shared by members of Phocoenidae and Monodontidae, while a 1 bp insertion in exon 1 was specific to Phocoenidae. A shared splice site mutation (AG→GG) was detected in Delphinidae, Phocoenidae, and Monodontidae. Additionally, a stop codon mutation was identified in the Indo-Pacific humpback dolphin. A 2 bp insertion in exon 2 and a splice site mutation in exon 7 were also detected in the Indus River dolphin. These mutations were confirmed by PCR amplification or raw read alignment (Figure 1). Collectively, these findings support the hypothesis that *TRPA1* underwent functional loss in the common ancestor of extant toothed whales.

TRPA1 in baleen whales

For baleen whales, protein-coding sequences of *TRPA1* were recovered in all species except the bowhead whale, for which exon 1 was missing (Figure 1; Supplementary Figure S1). Multiple splice site mutations were identified across the group. A GT→GC substitution at the 3' end of exon 7 was shared by all baleen whale species. Additional lineage-specific mutations were observed, including a GT→GA mutation at the 3' end of exon 3 in the Antarctic minke whale and two substitutions in the gray whale (GT→GC and GT→GG) at exons 2 and 6, respectively. A premature stop codon (TAG) was also detected in exon 2 of *TRPA1* in the fin whale. All mutations were validated by PCR or by alignment of raw sequencing reads (Figure 1). Notably, the exon 7 GT→GC splice site mutation, conserved across baleen whales, was also detected in the Indus River dolphin and the hippopotamus. To assess its evolutionary distribution, a broader comparison across 470 mammalian genomes was performed. Only 46 species retained the canonical GT splice donor site at this locus, while the GC variant was present in the remaining placental mammals (Supplementary Figure S2). The GT-retaining species included all 18 examined Metatheria, 16 Glires (e.g., mouse and rat), nine Camelidae, as well as the Hispaniolan solenodon, slow loris, and bushbaby. These findings suggest that the GC splice site at the 3' end of exon 7 predates the origin of cetaceans and may represent an ancestral state in certain eutherian lineages.

BLAST searches using *TRPA1* sequences from the blue whale, bowhead whale, Antarctic minke whale, and humpback

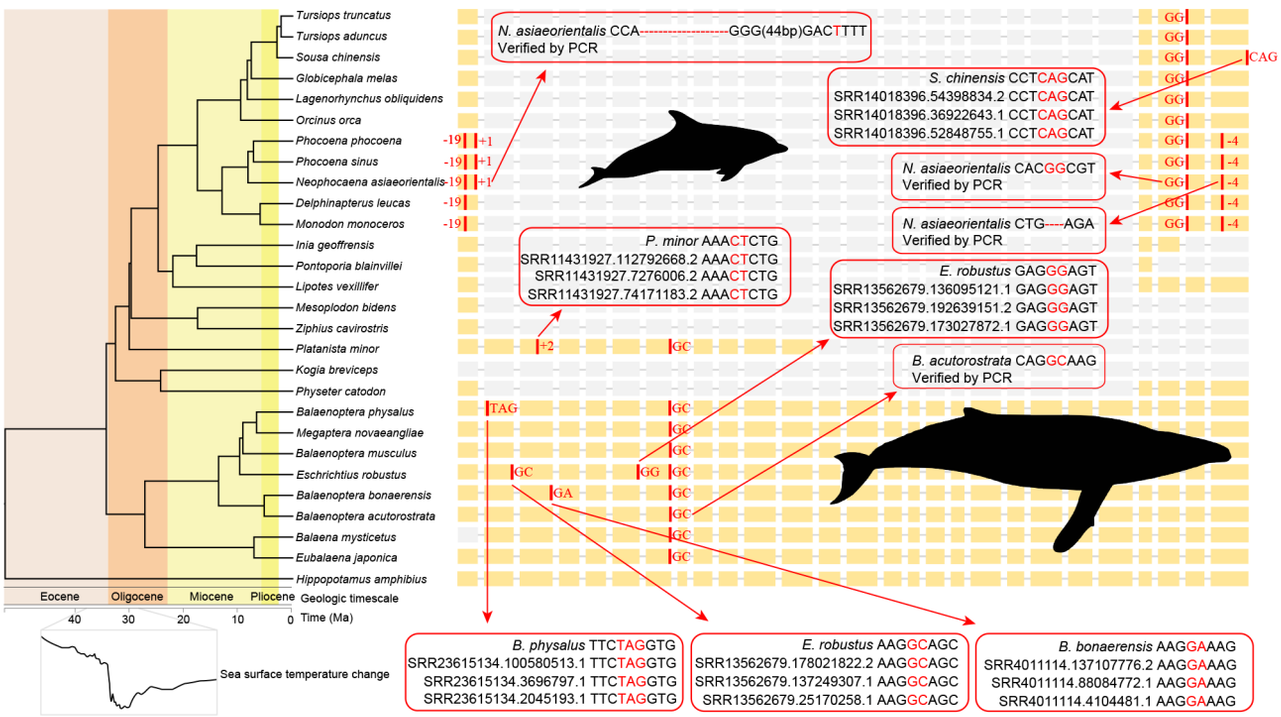

Figure 1 Inactivating mutations of *TRPA1* in cetacean lineages

Left panel shows phylogenetic relationship and divergence time based on McGowen et al. (2020) and data from TimeTree (https://timetree.org/). Sea surface temperature change curve was adapted from Liu et al. (2009). Right panel, yellow rectangles represent exons and gray rectangles represent missing exons. Red vertical lines denote mutations, including initiation codon mutations, stop codon mutations, frameshift insertions and deletions, and splice site mutations at the intron-exon boundary (GT/AG). Validation of inactivated mutations through read alignment or PCR is represented in red boxes.

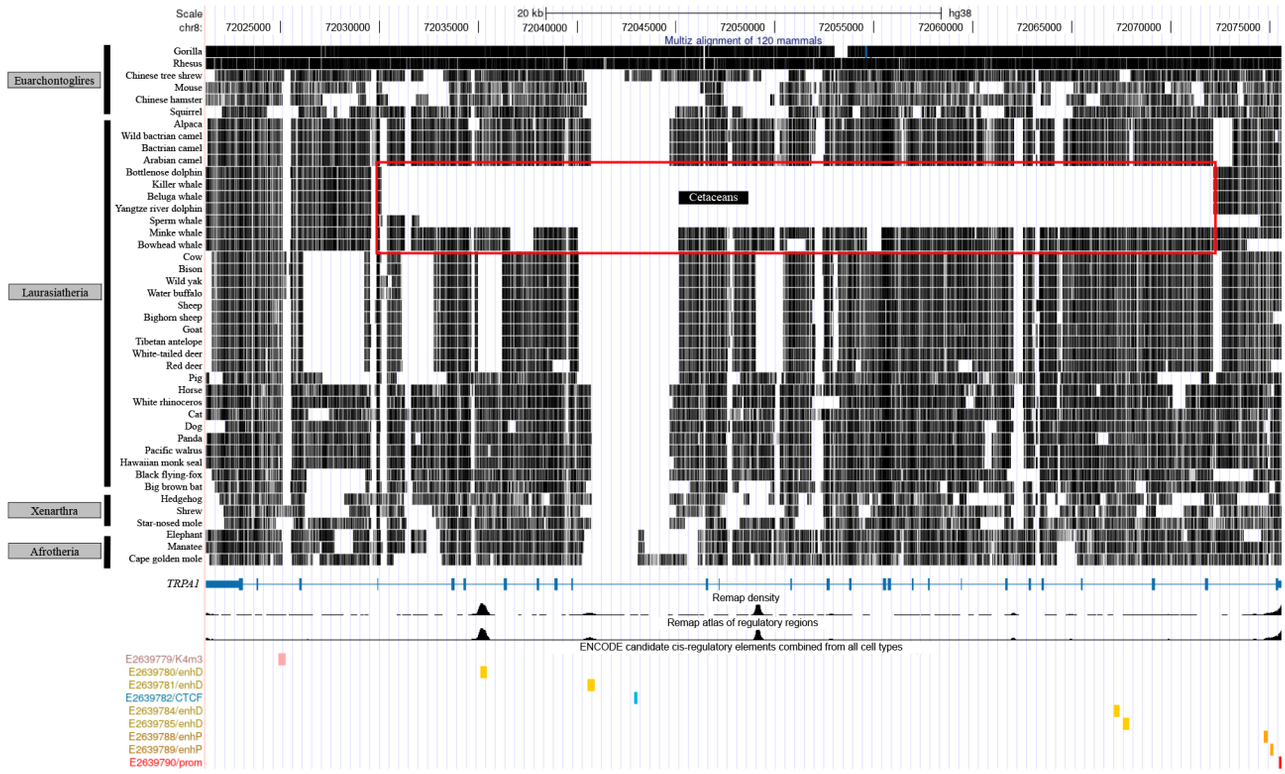

Figure 2 Genomic alignment of the *TRPA1* locus across representative mammalian lineages, visualized using the UCSC Genome Browser

Original genome alignment was based on Hecker & Hiller (2020), with the top scale representing genomic coordinates in the human reference genome (hg38). Main panel presents comparative alignment of *TRPA1* gene regions among representative species from Afrotheria, Euarchontoglires, Laurasiatheria, and Xenarthra. Red box highlights a large deletion in toothed whales, including a region spanning 22 exons, whereas baleen whales retain a complete gene structure. Blue regions indicate *TRPA1* exon-intron structures, with arrows denoting coding direction. Bottom panel illustrates potential regulatory roles of different genomic regions based on data from the ReMap and ENCODE databases: red indicates promoter-like signatures; yellow indicates distal enhancer-like signatures; blue indicates CTCF-only sites; pink indicates DNase-H3K4me3 regions.

whale as queries yielded few or no transcriptome matches across a range of baleen whale tissues, including skin, epidermis, blubber, muscle, cerebellum, liver, heart, brain, kidney, and lung (Figure 3). The highest number of matching reads was only 16, detected in a limited set of samples: skin and pooled tissue from the humpback whale, epidermis and blubber from the blue whale, and muscle, cerebellum, and liver from the bowhead whale. No *TRPA1* transcripts were detected in the remaining nine baleen whale transcriptomes. In contrast, *TRPA1* transcripts were clearly identified in the transcriptomes of the hippopotamus, as well as in the skin of cattle and humans, with 3 718, 496, and 548 reads obtained, respectively (Figure 3; Supplementary Table S3). These datasets were comparable in both library size and sequencing depth (Supplementary Table S3). These findings suggest that while *TRPA1* remains transcriptionally active in the terrestrial relatives of cetaceans, its expression in baleen whale tissues is markedly reduced or absent in most sampled contexts.

Given that baleen whales retain intact *TRPA1* coding sequences in contrast to the extensively disrupted loci observed in toothed whales, additional analyses were conducted to determine whether relaxed selective pressure may be acting on lineages with inactivating mutations. In branch model tests where three baleen whales carrying inactivating mutations were designated as the foreground, the estimated nonsynonymous-to-synonymous substitution rate increased (ω_b=0.23049, ω_f=0.53240), with a statistically significant difference relative to the null model assuming uniform selection across branches (*P*[Model A vs. B]=7.41×10^{-4}; Table 1). However, comparison with a model constraining the foreground branch to neutral evolution (ω=1) did not support a complete loss of selective constraint (*P*[Model C vs. B]=1.33×10^{-2}; Table 1). In contrast, when the five baleen whales without inactivating mutations were tested as the foreground branch, no significant difference in substitution rates was observed relative to background branches (ω_b=0.23248, ω_f=0.33020; P[Model A vs. D]=2.36×10^{-1}; Table 1). RELAX analysis similarly failed to detect evidence of relaxed selection, regardless of whether the foreground was assigned to whales with or without inactivating mutations (Figure 4A, B). Collectively, these findings suggest that the three baleen whales harboring inactivating mutations exhibited a modest relaxation of selective pressure, whereas the five whales without such mutations continued to evolve under purifying selection, despite the minimal expression detected in the sampled baleen whale transcriptomes.

In addition, a key amino acid residue within the S5 transmembrane domain, previously shown to influence interspecific variation in cold sensitivity (Chen et al., 2013), was examined across species. In baleen whales, this position (residue 877) was occupied by valine (877V), matching the variant found in primates, but differing from isoleucine in cattle (877I) and glycine in mice (877G) (Supplementary Figure S3).

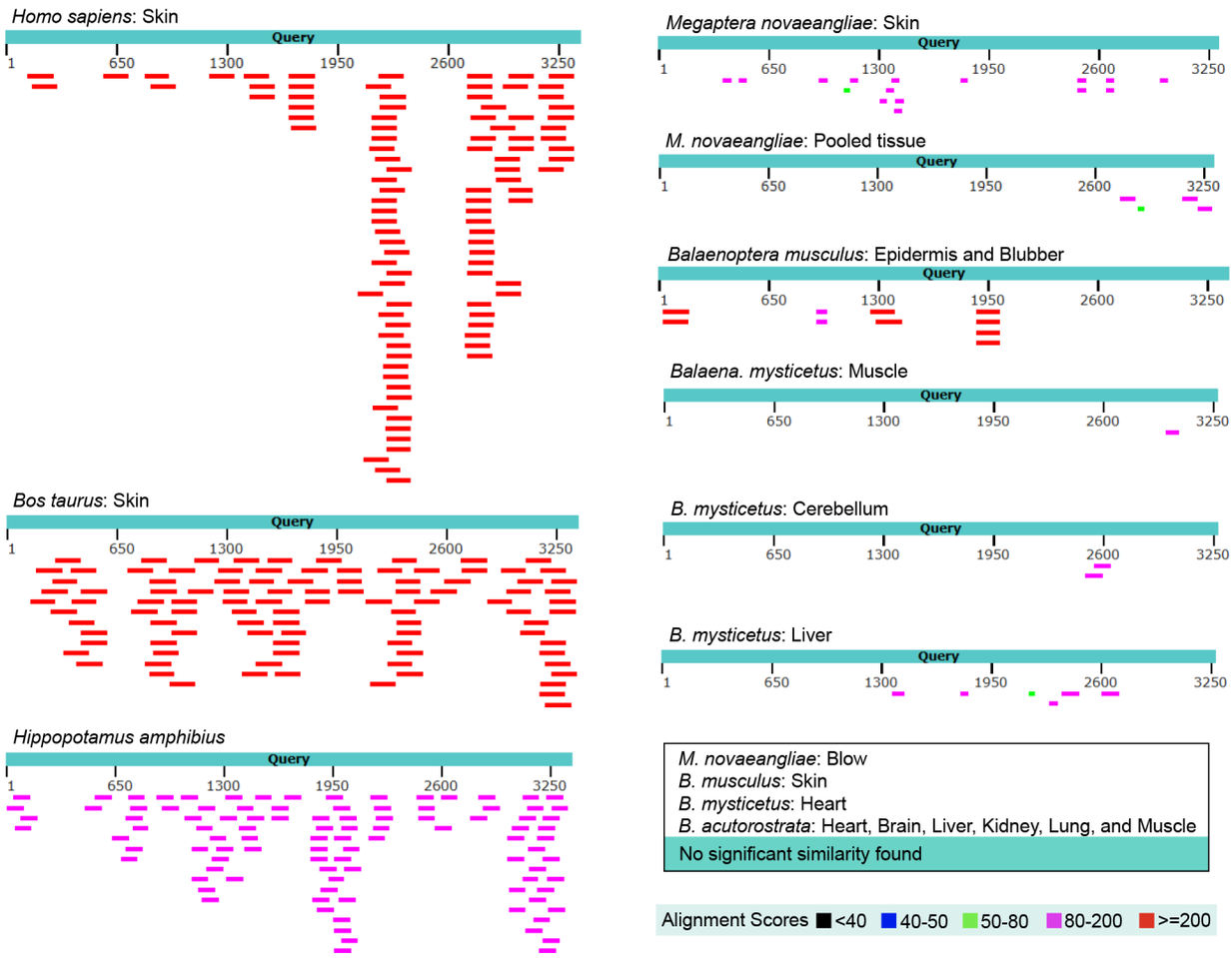

Figure 3 Transcriptomic mapping of *TRPA1* across selected species

For *H. sapiens*, *B. taurus*, and *H. amphibius*, only the top 100 BLAST hits are shown. In baleen whales, transcriptomic reads from six examined tissues yielded limited matches to *TRPA1*, as shown on the right. No alignments were detected in transcriptomic data from an additional nine tissues listed in Supplementary Table S3. Alignment scores are color-coded: green (50–80), purple (80–200), and red (>200), with higher scores indicating greater reliability.

DISCUSSION

The evolutionary transition of cetaceans from their terrestrial ancestor *Indohyus*—a small wading artiodactyl adapted to shallow water environments (Thewissen et al., 2007)—into a morphologically and ecologically diverse assemblage spanning marine and freshwater habitats represents a striking example of large-scale adaptive evolution (Gatesy et al., 2013). The present study demonstrated that *TRPA1* followed distinct evolutionary trajectories in toothed and baleen whales, a pattern that has implications for the modulation of thermosensation, nociception, skin physiology, and sensory specialization associated with aquatic life.

Comparative genomic analyses demonstrated that, with the exception of the Indus River dolphin, toothed whales shared extensive deletions spanning exons 2–23 of *TRPA1*, which encode nearly all transmembrane domains required for channel activity (Figure 1). This conserved deletion pattern supports functional loss of *TRPA1* in the common ancestor of odontocetes. In contrast, baleen whales retained intact *TRPA1* coding sequences, yet transcriptomic surveys across multiple tissues detected little to no expression. Together, these observations indicate that *TRPA1* lost protein-coding capacity in toothed whales and experienced marked functional attenuation in baleen whales. The genomic segment absent in toothed whales but retained in baleen whales encompassed two putative regulatory regions identified by the ReMap database and three candidate cis-regulatory elements annotated in the ENCODE database (Figure 2), one of which was recognized by both databases. Although these elements have yet to be experimentally validated, bioinformatic analyses of 706 human DNase-seq datasets indicated that all three ENCODE-annotated regions exhibited features characteristic of distal enhancers (The ENCODE Project Consortium et al., 2020). Retention of these noncoding elements suggests that regulatory constraints may contribute to preservation of intronic regions within *TRPA1* despite loss or attenuation of protein-coding function. Such an interpretation is consistent with growing evidence that pseudogenized loci can retain or acquire regulatory roles; for example, the human η-globin pseudogene plays an essential role in erythropoiesis through a lineage-specific regulatory mechanism (Ma et al., 2021). Overall, these findings expand the catalog of cetacean gene loss and provide a potential molecular basis for their adaptive evolution.

A single amino acid substitution within the S5 transmembrane domain—valine in humans and glycine in mice—determines *TRPA1* cold sensitivity, with mouse *TRPA1* being responsive to cold stimuli, whereas the human ortholog

Table 1 Results of selection analyses based on five branch models

Models	Foreground branch	ω	lnL	np	Models compared	2Δ (ln L)	*P*-value
A: One ratio		0.23329	−29 393.60791	72			
B: Two ratio	Three baleen whales with inactivating mutation	ω_b=0.23049 ω_f=0.53240	−29 387.91579	73	A vs. B	11.384248	7.41E-04
C: Two ratio (ω=1)	Three baleen whales with inactivating mutation	ω_b=0.23062 ω_f=1	−29 390.9793	72	C vs. B	6.127018	1.33E-02
D: Two ratio	Five baleen whales without inactivating mutation	ω_b=0.23248 ω_f=0.33020	−29 392.90517	73	A vs. D	1.405492	2.36E-01
E: Two ratio (ω=1)	Five baleen whales without inactivating mutation	ω_b=0.23266 ω_f=1	−29 399.86637	72	E vs. D	13.922394	1.91E-04

Model A represents the null hypothesis. Models B and D (alternative hypotheses) specify foreground branches comprising three baleen whales with inactivating mutations and five baleen whales without inactivating mutations, respectively. Models C and E are derived from Models B and D, but with the ω value fixed at 1. Likelihood ratio tests comparing A vs. B and A vs. D assessed whether foreground lineages exhibited signals of accelerated evolution, while C vs. B and E vs. D tested for relaxed selection in those lineages. lnL indicates log-likelihood calculated by PAML; np denotes number of parameters.

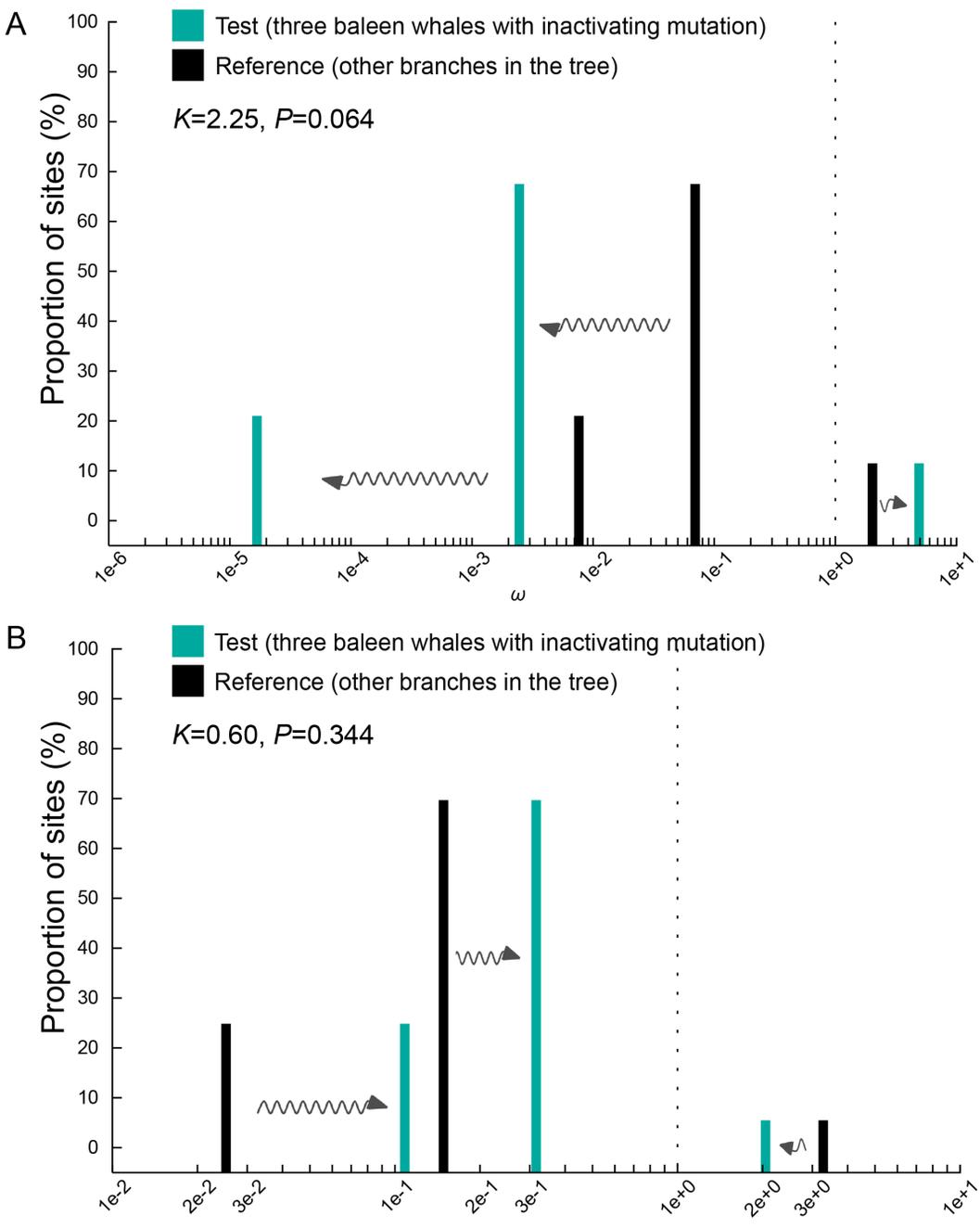

Figure 4 Selection pressure analysis in baleen whales using RELAX

Plot displays three ω values (horizontal axis) and their relative site proportions (vertical axis) for test branches (green) and reference branches (black). A, B: Gray dashed vertical lines represent neutral evolution. Tests were conducted using three baleen whales with inactivating mutations and five without, designated as foreground branches. Results indicate that these lineages are not under relaxed selection.

is not (Chen et al., 2013). The homologous site (877V) in baleen whales is consistent with that in primates (Supplementary Figure S3), potentially indicating a conserved insensitivity to temperature. However, additional studies employing DRG neurons, HEK293 cells, and oocytes have reported cold-induced activation of human *TRPA1* (Zhang et al., 2022), revealing conflicting evidence regarding its thermosensitivity. These inconsistencies highlight the limitations of inferring functional phenotypes from single residues in isolation. Therefore, one possibility is that the loss of 21 exons in toothed whales, along with the relatively low expression levels observed in baleen whales, may have led to the functional inactivation of *TRPA1*, potentially as an adaptation to changes in ambient temperature. This evolutionary trajectory may have been shaped by the Eocene-Oligocene transition (approximately 34 Ma), a period of significant climatic cooling and widespread faunal turnover, including the decline of archaeocete lineages (Hull, 2015; Ivany et al., 2000). Phylogenomic analyses date the divergence of odontocetes and mysticetes to approximately 36Ma (McGowen et al., 2020), placing the origin of these clades within the context of this global environmental shift. Disruption of thermosensory genes such as *TRPA1* typically alters temperature detection thresholds and downstream sensory signaling. *TRPA1* knockout mice exhibit impaired cold perception, as indicated by reduced cold-evoked jumping and a lower frequency of cold-responsive neurons compared to wild-type controls (Fajardo et al., 2008; Karashima et al., 2009). Functional loss of *TRPA1* in toothed whales may have similarly modulated thermal responsiveness, potentially conferring adaptive benefits in changing marine habitats. *TRPA1* transcripts were detected at low levels in extant species such as the blue whale, bowhead whale, and humpback whale, and absent in all six transcriptomes of the common minke whale, implying an overall reduction in *TRPA1* activity. However, whether their common ancestor maintained robust *TRPA1* expression remains unresolved. Although the Eocene-Oligocene boundary represents a significant global cooling event, our current evidence cannot determine whether the functional loss of *TRPA1* in toothed whales occurred immediately after their divergence or after a considerable temporal gap. Most toothed whales inhabit lower latitudes, while baleen whales are capable of living in higher-latitude environments and tolerating a broader temperature range. These contrasting thermal environments likely imposed distinct selective pressures on each lineage, shaping their divergent evolutionary trajectories at this locus.

Loss of *TRPA1* may have contributed to diminished pain perception in cetaceans. This channel is directly activated by a broad range of inflammatory factors, including reactive oxygen species, nitric oxide, and cyclopentenone prostaglandins, thereby playing a central role in acute pain signaling (Souza et al., 2020). In Schwann cells, nerve injury induces oxidative stress that triggers *TRPA1*-dependent release of H_2O_2, which, in turn, activates nociceptors and provokes mechanical allodynia. Following their secondary transition to aquatic life, cetaceans were exposed to a variety of pain-related stressors, including ultraviolet-induced and diving-related oxidative stress, both capable of eliciting endogenous nociceptive responses. In addition, contact between open wounds and high-salinity seawater may exacerbate pain; nevertheless, bottlenose dolphins exhibit a striking insensitivity to injury-associated discomfort (Zasloff, 2011). In recent years, *TRPA1* has attracted growing interest as a therapeutic target for analgesic drug development in humans (Souza et al., 2020), suggesting that its loss in cetaceans may reflect an adaptive modulation of pain pathways. Functional inactivation of *TRPA1* may have raised their nociceptive thresholds, particularly under conditions of environmental insult, endogenous inflammatory responses, or traumatic interactions. Convergent shifts in pain perception have also been documented in other species. For instance, the African naked mole-rat is insensitive to acid-induced pain, while the pallid bat, a predator of venomous scorpions, exhibits high tolerance to sting-induced pain. These phenotypes have been linked to mutations in *TRKA* and *NAV1.7*, respectively (Hopp et al., 2017; Omerbašić et al., 2016). In addition to *TRPA1*, multiple pseudogenized nociception-associated genes and positively selected analgesia-related genes have been identified in cetaceans (Ding et al., 2022), underscoring the evolutionary remodeling of pain pathways in response to the distinctive demands of marine life.

Gene loss can drive morphological evolution by eliminating traits that are no longer beneficial, thereby facilitating structural and functional adaptations. The inactivation of *TRPA1* may relate to the distinctive epidermal architecture of cetaceans, which includes a markedly thickened stratum spinosum, absence of the granular layer, and incomplete keratinization. *TRPA1* is expressed in human keratinocytes, melanocytes, and fibroblasts, and functions in melanocyte-mediated extraocular phototransduction (Bellono et al., 2013). In murine skin, application of a *TRPA1* agonist has been shown to accelerate lamellar body secretion at the stratum corneum-granular layer interface, facilitating rapid barrier regeneration (Denda et al., 2010). Given the evolution of a hyperplastic epidermis in cetaceans, the barrier-related function of *TRPA1* may have become redundant, akin to keratin-associated genes, thus escaping selective constraint. At the genomic level, widespread loss of *TRPA1* in toothed whales may also be linked to the emergence of echolocation. In mice, *TRPA1* mediates astrocyte-initiated neuromodulatory responses to low-intensity, low-frequency ultrasound (Oh et al., 2019), while in humans, it confers ultrasound sensitivity to mammalian cells (Duque et al., 2022). These studies suggest that *TRPA1* is closely associated with ultrasonic detection. Toothed whales possess a highly specialized nasal complex for sound generation and have evolved sophisticated echolocation, accompanied by positive selection on genes implicated in this sensory modality (Magpali et al., 2024; Shen et al., 2012). Although *TRPA1* is retained in baleen whales, its complete absence in toothed whales suggests functional incompatibility or dispensability during the evolution of echolocation in this lineage.

Two salient patterns emerged from our analysis of *TRPA1* sequence evolution. First, the Indus River dolphin retained more than a dozen *TRPA1* exons (Figure 1), an unexpected feature among toothed whales. This pattern is consistent with at least two evolutionary scenarios: independent loss events within odontocetes, or a stepwise deletion process in which exons 13–23 were eliminated in the stem lineage, followed by a subsequent loss of exons 2–12 in most descendant lineages. The retained exons in the Indus River dolphin are unlikely to reflect contamination or introgression from baleen whales, as the sequence contained a unique 2 bp insertion in exon 3 and multiple lineage-specific substitutions absent in all other baleen whale species. Second, a splice site mutation at

the 3' end of exon 7 (GT→GC) was identified across all placental mammals, indicating that this variant alone cannot account for the relatively low expression of *TRPA1* in baleen whales. GC donor sites are the most common non-canonical splice sites in mammalian genomes and are known to play important roles in regulating gene expression (Burset et al., 2000; Churbanov et al., 2008; Hiller et al., 2006). This suggests a deep evolutionary shift in *TRPA1* regulation early in placental mammal evolution. Notably, reversion to the canonical GT donor was observed in 28 placental species, including mice and rats, implying potential lineage-specific adaptive significance at this locus, particularly within rodents.

Across vertebrates, *TRPA1* displays pronounced functional and structural plasticity. Large-scale deletion of this gene in toothed whales and markedly reduced expression in several baleen whales together indicate substantial divergence of *TRPA1* function in cetaceans, although precise physiological roles remain unclear. Several evolutionary scenarios may account for this unique trajectory, collectively pointing to lineage-specific remodeling of sensory and regulatory pathways during adaptation to aquatic environments.

SUPPLEMENTARY DATA

Supplementary data to this article can be found online.

COMPETING INTERESTS

The authors declare that they have no competing interests.

AUTHORS' CONTRIBUTIONS

G.Y. and S.X.X. made substantial contributions to the concept and design of the study. T.Z.W., X.T.H., and Y.Q.D. were responsible for data acquisition, analysis, and interpretation. L.Y.D. conducted the experiments. T.Z.W. drafted the manuscript, while G.Y., S.X.X., and T.Z.W. critically revised its intellectual content. G.Y. had the final authority for article approval. All authors read and approved the final version of the manuscript.

ACKNOWLEDGMENTS

We thank members of the Jiangsu Key Laboratory for Biodiversity and Biotechnology, Nanjing Normal University, for their contributions to this paper. In particular, we extend special thanks to Dr. Zhen-Peng Yu and Dr. Xin Huang for technical support and helpful discussion. We are thankful to Dr. Ran Tian and Dr. Si-Min Chai for their insightful discussion. We sincerely thank the five reviewers for their constructive comments.

REFERENCES

Altschul SF, Gish W, Miller W, et al. 1990. Basic local alignment search tool. *Journal of Molecular Biology*, **215**(3): 403–410.

Andersson DA, Gentry C, Moss S, et al. 2008. Transient receptor potential A1 is a sensory receptor for multiple products of oxidative stress. *Journal of Neuroscience*, **28**(10): 2485–2494.

Balemans D, Boeckxstaens GE, Talavera K, et al. 2017. Transient receptor potential ion channel function in sensory transduction and cellular signaling cascades underlying visceral hypersensitivity. *American Journal of Physiology-Gastrointestinal and Liver Physiology*, **312**(6): G635–G648.

Bautista DM, Jordt SE, Nikai T, et al. 2006. TRPA1 mediates the inflammatory actions of environmental irritants and proalgesic agents. *Cell*, **124**(6): 1269–1282.

Bellono NW, Kammel LG, Zimmerman AL, et al. 2013. UV light phototransduction activates transient receptor potential A1 ion channels in human melanocytes. *Proceedings of the National Academy of Sciences of the United States of America*, **110**(6): 2383–2388.

Benemei S, Fusi C, Trevisan G, et al. 2014. The TRPA1 channel in migraine mechanism and treatment. *British Journal of Pharmacology*, **171**(10): 2552–2567.

Bukhman YV, Morin PA, Meyer S, et al. 2024. A high-quality blue whale genome, segmental duplications, and historical demography. *Molecular Biology and Evolution*, **41**(3): msae036.

Burset M, Seledtsov IA, Solovyev VV. 2000. Analysis of canonical and non-canonical splice sites in mammalian genomes. *Nucleic Acids Research*, **28**(21): 4364–4375.

Castresana J. 2000. Selection of conserved blocks from multiple alignments for their use in phylogenetic analysis. *Molecular Biology and Evolution*, **17**(4): 540–552.

Chai SM, Kang JQ, Wu TZ, et al. 2024. Coevolution and adaptation of transition nuclear proteins and protamines in naturally ascrotal mammals support the Black Queen Hypothesis. *Genome Biology and Evolution*, **16**(12): evae260.

Chen J. 2015. The evolutionary divergence of TRPA1 channel: heat-sensitive, cold-sensitive and temperature-insensitive. *Temperature*, **2**(2): 158–159.

Chen J, Kang D, Xu J, et al. 2013. Species differences and molecular determinant of TRPA1 cold sensitivity. *Nature Communications*, **4**: 2501.

Churbanov A, Winters-Hilt S, Koonin EV, et al. 2008. Accumulation of GC donor splice signals in mammals. *Biology Direct*, **3**: 30.

Delmas P, Hao JZ, Rodat-Despoix L. 2011. Molecular mechanisms of mechanotransduction in mammalian sensory neurons. *Nature Reviews Neuroscience*, **12**(3): 139–153.

Denda M, Tsutsumi M, Goto M, et al. 2010. Topical application of TRPA1 agonists and brief cold exposure accelerate skin permeability barrier recovery. *Journal of Investigative Dermatology*, **130**(7): 1942–1945.

Ding XY, Yu FF, He XF, et al. 2022. Rubbing salt in the wound: molecular evolutionary analysis of pain-related genes reveals the pain adaptation of cetaceans in seawater. *Animals*, **12**(24): 3571.

Duque M, Lee-Kubli CA, Tufail Y, et al. 2022. Sonogenetic control of mammalian cells using exogenous Transient Receptor Potential A1 channels. *Nature Communications*, **13**(1): 600.

Edgar RC. 2004. MUSCLE: a multiple sequence alignment method with reduced time and space complexity. *BMC Bioinformatics*, **5**: 113.

Fajardo O, Meseguer V, Belmonte C, et al. 2008. TRPA1 channels mediate cold temperature sensing in mammalian vagal sensory neurons: pharmacological and genetic evidence. *Journal of Neuroscience*, **28**(31): 7863–7875.

Feng P, Zheng JS, Rossiter SJ, et al. 2014. Massive losses of taste receptor genes in toothed and baleen whales. *Genome Biology and Evolution*, **6**(6): 1254–1265.

Figuet E, Ballenghien M, Lartillot N, et al. 2021. Reconstruction of body mass evolution in the Cetartiodactyla and mammals using phylogenomic data. *Peer Community Journal*, **1**: e42.

Gai YL, Tian R, Liu FN, et al. 2023. Diversified mammalian visual adaptations to bright- or dim-light environments. *Molecular Biology and Evolution*, **40**(4): msad063.

Gatesy J, Geisler JH, Chang J, et al. 2013. A phylogenetic blueprint for a modern whale. *Molecular Phylogenetics and Evolution*, **66**(2): 479–506.

Geng J, Liang D, Jiang K, et al. 2011. Molecular evolution of the infrared sensory gene TRPA1 in snakes and implications for functional studies. *PLoS One*, **6**(12): e28644.

Geoghegan JL, Pirotta V, Harvey E, et al. 2018. Virological sampling of inaccessible wildlife with drones. *Viruses*, **10**(6): 300.

Gracheva EO, Ingolia NT, Kelly YM, et al. 2010. Molecular basis of infrared detection by snakes. *Nature*, **464**(7291): 1006–1011.

Guo BX, Zhang Y, Sun XY, et al. 2024. Convergent evolution in high-altitude and marine mammals: Molecular adaptations to pulmonary fibrosis and hypoxia. *Zoological Research*, **45**(6): 1209–1220.

Hecker N, Hiller M. 2020. A genome alignment of 120 mammals highlights

ultraconserved element variability and placenta-associated enhancers. *Gigascience*, **9**(1): giz159.

Hiller M, Huse K, Szafranski K, et al. 2006. Phylogenetically widespread alternative splicing at unusual GYNGYN donors. *Genome Biology*, **7**(7): R65.

Hopp BH, Arvidson RS, Adams ME, et al. 2017. Arizona bark scorpion venom resistance in the pallid bat, *Antrozous pallidus*. *PLoS One*, **12**(8): e0183215.

Horwitz SM, Nirmal AJ, Rahman J, et al. 2024. Duvelisib plus romidepsin in relapsed/refractory T cell lymphomas: a phase 1b/2a trial. *Nature Medicine*, **30**(9): 2517–2527.

Hou SM, Wu HT, Chen S, et al. 2022. Bovine skin fibroblasts mediated immune responses to defend against bovine *Acinetobacter baumannii* infection. *Microbial Pathogenesis*, **173**: 105806.

Huang X, Sun D, Wu TZ, et al. 2021. Genomic insights into body size evolution in Carnivora support Peto's paradox. *BMC Genomics*, **22**(1): 429.

Huelsmann M, Hecker N, Springer MS, et al. 2019. Genes lost during the transition from land to water in cetaceans highlight genomic changes associated with aquatic adaptations. *Science Advances*, **5**(9): eaaw6671.

Hull P. 2015. Life in the aftermath of mass extinctions. *Current Biology*, **25**(19): R941–R952.

Ivany LC, Patterson WP, Lohmann KC. 2000. Cooler winters as a possible cause of mass extinctions at the Eocene/Oligocene boundary. *Nature*, **407**(6806): 887–890.

Karashima Y, Talavera K, Everaerts W, et al. 2009. TRPA1 acts as a cold sensor in vitro and in vivo. *Proceedings of the National Academy of Sciences of the United States of America*, **106**(4): 1273–1278.

Keane M, Semeiks J, Webb AE, et al. 2015. Insights into the evolution of longevity from the bowhead whale genome. *Cell Reports*, **10**(1): 112–122.

Kishida T, Thewissen JGM, Hayakawa T, et al. 2015. Aquatic adaptation and the evolution of smell and taste in whales. *Zoological Letters*, **1**: 9.

Kodama Y, Shumway M, Leinonen R. 2012. The sequence read archive: explosive growth of sequencing data. *Nucleic Acids Research*, **40**(D1): D54–D56.

Kumar S, Stecher G, Tamura K. 2016. MEGA7: molecular evolutionary genetics analysis version 7.0 for bigger datasets. *Molecular Biology and Evolution*, **33**(7): 1870–1874.

Kwan KY, Allchorne AJ, Vollrath MA, et al. 2006. TRPA1 contributes to cold, mechanical, and chemical nociception but is not essential for hair-cell transduction. *Neuron*, **50**(2): 277–289.

Liang N, Deme LY, Kong Q, et al. 2022. Divergence of *Tbx4* hindlimb enhancer HLEA underlies the hindlimb loss during cetacean evolution. *Genomics*, **114**(2): 110292.

Liu ZH, Pagani M, Zinniker D, et al. 2009. Global cooling during the Eocene-Oligocene climate transition. *Science*, **323**(5918): 1187–1190.

Lopes-Marques M, Machado AM, Alves LQ, et al. 2019. Complete inactivation of sebum-producing genes parallels the loss of sebaceous glands in Cetacea. *Molecular Biology and Evolution*, **36**(6): 1270–1280.

Löytynoja A. 2013. Phylogeny-aware alignment with PRANK. *In*: Russell DJ. Multiple Sequence Alignment Methods. Totowa: Humana, 155–170.

Ma YN, Liu SQ, Gao J, et al. 2021. Genome-wide analysis of pseudogenes reveals *HBBP1*'s human-specific essentiality in erythropoiesis and implication in β-thalassemia. *Developmental Cell*, **56**(4): 478–493. e11.

Maglie R, Souza Monteiro de Araujo D, Antiga E, et al. 2021. The role of TRPA1 in skin physiology and pathology. *International Journal of Molecular Sciences*, **22**(6): 3065.

Magpali L, Ramos E, Picorelli A, et al. 2024. Molecular evolution of toothed whale genes reveals adaptations to echolocating in different environments. *BMC Genomics*, **25**(1): 1049.

McGowen MR, Tsagkogeorga G, Álvarez-Carretero S, et al. 2020. Phylogenomic resolution of the cetacean tree of life using target sequence capture. *Systematic Biology*, **69**(3): 479–501.

Meents JE, Ciotu CI, Fischer MJM. 2019. TRPA1: a molecular view. *Journal of Neurophysiology*, **121**(2): 427–443.

Minkin I, Salzberg SL. 2025. Conservation assessment of human splice site annotation based on a 470-genome alignment. *Nucleic Acids Research*, **53**(6): gkaf184.

Moore C, Gupta R, Jordt SE, et al. 2018. Regulation of pain and itch by TRP channels. *Neuroscience Bulletin*, **34**(1): 120–142.

Mu Y, Huang X, Liu R, et al. 2021. *ACPT* gene is inactivated in mammalian lineages that lack enamel or teeth. *PeerJ*, **9**: e10219.

Nagata K, Duggan A, Kumar G, et al. 2005. Nociceptor and hair cell transducer properties of TRPA1, a channel for pain and hearing. *Journal of Neuroscience*, **25**(16): 4052–4061.

Nilius B, Appendino G, Owsianik G. 2012. The transient receptor potential channel TRPA1: from gene to pathophysiology. *Pflügers Archiv-European Journal of Physiology*, **464**(5): 425–458.

Oh SJ, Lee JM, Kim HB, et al. 2019. Ultrasonic neuromodulation via astrocytic TRPA1. *Current Biology*, **29**(20): 3386–3401. e8.

Omerbašić D, Smith ESJ, Moroni M, et al. 2016. Hypofunctional TrkA accounts for the absence of pain sensitization in the African naked mole-rat. *Cell Reports*, **17**(3): 748–758.

Randall JG, Gatesy J, Springer MS. 2022. Molecular evolutionary analyses of tooth genes support sequential loss of enamel and teeth in baleen whales (Mysticeti). *Molecular Phylogenetics and Evolution*, **171**: 107463.

Saito S, Saito CT, Igawa T, et al. 2022. Evolutionary tuning of transient receptor potential Ankyrin 1 underlies the variation in heat avoidance behaviors among frog species inhabiting diverse thermal niches. *Molecular Biology and Evolution*, **39**(9): msac180.

Shen YY, Liang L, Li GS, et al. 2012. Parallel evolution of auditory genes for echolocation in bats and toothed whales. *PLoS Genetics*, **8**(6): e1002788.

Souza Monteiro de Araujo D, Nassini R, Geppetti P, et al. 2020. TRPA1 as a therapeutic target for nociceptive pain. *Expert Opinion on Therapeutic Targets*, **24**(10): 997–1008.

Springer MS, Guerrero-Juarez CF, Huelsmann M, et al. 2021. Genomic and anatomical comparisons of skin support independent adaptation to life in water by cetaceans and hippos. *Current Biology*, **31**(10): 2124–2139. e3.

The ENCODE Project Consortium, Moore JE, Purcaro MJ, et al. 2020. Expanded encyclopaedias of DNA elements in the human and mouse genomes. *Nature*, **583**(7818): 699–710.

Themudo GE, Ruivo R, Valente R, et al. 2025. Gene Loss DB: a curated database for gene loss in vertebrate species. *BioRxiv*. doi: https://doi.org/10.1101/2025.05.26.656173.

Thewissen JGM, Cooper LN, Clementz MT, et al. 2007. Whales originated from aquatic artiodactyls in the Eocene Epoch of India. *Nature*, **450**(7173): 1190–1194.

Tollis M, Robbins J, Webb AE, et al. 2019. Return to the sea, get huge, beat cancer: an analysis of cetacean genomes including an assembly for the humpback whale (*Megaptera novaeangliae*). *Molecular Biology and Evolution*, **36**(8): 1746–1763.

Tsagkogeorga G, McGowen MR, Davies KTJ, et al. 2015. A phylogenomic analysis of the role and timing of molecular adaptation in the aquatic transition of cetartiodactyl mammals. *Royal Society Open Science*, **2**(9): 150156.

Uhen MD. 2010. The origin(s) of whales. *Annual Review of Earth and Planetary Sciences*, **38**: 189–219.

Vélez-Ortega AC, Stepanyan R, Edelmann SE, et al. 2023. TRPA1 activation in non-sensory supporting cells contributes to regulation of cochlear sensitivity after acoustic trauma. *Nature Communications*, **14**(1): 3871.

Vriens J, Nilius B, Voets T. 2014. Peripheral thermosensation in mammals. *Nature Reviews Neuroscience*, **15**(9): 573–589.

Wertheim JO, Murrell B, Smith MD, et al. 2015. RELAX: detecting relaxed selection in a phylogenetic framework. *Molecular Biology and Evolution*, **32**(3): 820–832.

Wilson SR, Nelson AM, Batia L, et al. 2013. The ion channel TRPA1 is required for chronic itch. *Journal of Neuroscience*, **33**(22): 9283–9294.

Wu TZ, Deme LY, Zhang ZH, et al. 2022. Decay of *TRPV3* as the genomic trace of epidermal structure changes in the land‐to‐sea transition of mammals. *Ecology and Evolution*, **12**(3): e8731.

Xu SX, Shan L, Tian R, et al. 2025. Multi-level genomic convergence of secondary aquatic adaptation in marine mammals. *The Innovation*, **6**(3): 100798.

Yan CC, Wu W, Dong WQ, et al. 2022. Temperature acclimation in hot-spring snakes and the convergence of cold response. *The Innovation*, **3**(5): 100295.

Yang ZH. 2007. PAML 4: phylogenetic analysis by maximum likelihood. *Molecular Biology and Evolution*, **24**(8): 1586–1591.

Yim HS, Cho YS, Guang XM, et al. 2014. Minke whale genome and aquatic adaptation in cetaceans. *Nature Genetics*, **46**(1): 88–92.

Yu ZP, Seim I, Yin MX, et al. 2021. Comparative analyses of aging-related genes in long-lived mammals provide insights into natural longevity. *The Innovation*, **2**(2): 100108.

Zasloff M. 2011. Observations on the remarkable (and mysterious) wound-healing process of the bottlenose dolphin. *Journal of Investigative Dermatology*, **131**(12): 2503–2505.

Zhang F, Zhang T, Dong H, et al. 2025. Comparative genomics uncovers molecular adaptations for cetacean deep-sea diving. *Molecular Ecology*, doi: 10.1111/mec.17678.

Zhang H, Wang CS, Zhang KY, et al. 2022. The role of TRPA1 channels in thermosensation. *Cell Insight*, **1**(6): 100059.

Zhou M, Wu TZ, Chen Y, et al. 2022. Functional attenuation of *UCP1* as the potential mechanism for a thickened blubber layer in cetaceans. *Molecular Biology and Evolution*, **39**(11): msac230.